ISSN 0036-0244, Russian Journal of Physical Chemistry A, 2020, Vol. 94, No. 1, pp. 143–151. © Pleiades Publishing, Ltd., 2020.

Experimental Spectroscopic and Theoretical Studies of New Synthesized Sulfonamide Derivatives

M. T. Bilkan[a],*, S. Alyar[b], and H. Alyar[a]

[a] *Department of Physics, Faculty of Science, Çankırı Karatekin University, Çankırı, 18100 Turkey*

[b] *Department of Chemistry, Faculty of Science, Çankırı Karatekin University, Çankırı, 18100 Turkey*

**e-mail: mtbilkan@gmail.com*

Received January 21, 2019; revised April 24, 2019; accepted June 18, 2019

Abstract—In this paper, two new Schiff bases (L_1 and L_2) derived from substituted salicylaldehyde and sulfamethoxazole/sulfisoxazole were synthesized. The synthesized structures were elucidated by experimental spectroscopic methods such as FT-IR, ^{1}H-^{13}C NMR, ^{1}H, and ^{13}C shielding tensors, and elemental analysis. The theoretical vibrational modes and nonlinear optical (NLO) properties have been computed by DFT/B3LYP/6-311G(*d,p*) method. Theoretical ^{1}H and ^{13}C shielding tensors were calculated with GIAO methods in $CDCl_3$ with same level of theory. The results have shown that there is perfect harmony between the calculated parameters and recorded experimental data. The first order hyperpolarizabilities of the new synthesized compounds are 201.79 and 113.14 times larger than that of urea (0.3728×10^{-30} esu), respectively. According to evaluated results, the L_1 and L_2 present large nonlinear optical activity and are candidate molecules for nonlinear optical applications.

Keywords: sulfonamide derivatives, spectroscopic and theoretical studies, Schiff bases

DOI: 10.1134/S0036024420010045

INTRODUCTION

Sulfonamides together with various pharmacological agents with antibacterial, anti-carbonic anhydrase, diuretic, and hypoglycemic activities constitute a significant group of drugs. With the progressivity in the technology and analysis techniques, considerable influences of sulfonamides in living tissue have been elucidated. Sulfonamide and its derivatives have multifunctional chemistry and so interests are increasing has been made to synthesize the new Schiff base ligands and its complexes. [1]. The enzyme, which has the strongest inhibitory effect of sulfonamides, is known as carbonic anhydrase (CA). This enzyme is found in plants, animals and humans; it catalyzes the conversion of carbonic acid to carbon dioxide. Numerous studies have been conducted on the inhibition of carbonic anhydrase enzyme and the treatment of diseases such as diuretic, glaucoma, epilepsy, acute mountain sickness and obesity and cancer in recent years [2–8]. Additionally, Schiff bases and complexes from commercial drugs of sulfamethoxazole and sulfoxazoline have been investigated in terms of biological activity in many studies.

In our previous papers, different sulfonamides were synthesized and antimicrobial activities of the compounds were investigated [9–12]. Moreover, structural and spectroscopic properties of methanesulfonic acid hydrazide, [13] methanesulfonic acid 1-methylhydrazide [14] and some methanesulfonylhydrazone derivatives were also studied with the conformation analysis of them [15, 16]. In this paper, two new Schiff bases compound have been synthesized since the above-mentioned importance. Synthesized compounds were named as (2E)-2-[4-(dimethylamino)phenyl]-2-({4-[(4-methanediidyl-5-methyl-2H-1λ^3,2-oxazol-2-id-3-yl)sulfamoyl]phenyl}imino)ethane-1,1-diide (L_1) and (2E)-2-({4-[(3,4-dimethyl-1,2-oxazol-5-yl)sulfamoyl]phenyl}imino)-2-[4-(dimethylamino)phenyl]ethane-1,1-diide (L_2). They were derived from sulfamethoxazole (S1)/sulfisoxazole (S2) and substituted salicylaldehyde. Synthesized compounds have been characterized by using elemental analyses, FT-IR and ^{1}H–^{13}C NMR methods. The theoretical vibrational modes and nonlinear optical (NLO) activity have been investigated by B3LYP/6-311G(*d,p*) level of theory. ^{1}H and ^{13}C NMR calculations of the compounds were performed with GIAO/DFT/B3LYP/6-311G(*d,p*) methods in $CDCl_3$.

Table 1. The C, H, N, and S analyses of the compounds

Compound	C, %	H, %	N, %	S, %
L_1 (calc.)	59.85 (59.36)	5.21 (5.24)	14.25 (14.57)	8.58 (8.34)
L_2 (calc.)	60.85 (60.28)	5.21 (5.56)	14.25 (14.06)	8.58 (8.05)

EXPERIMENTAL

Synthesis and Spectroscopic Measurements of the Compounds

The general method of synthesis of Schiff bases is as follows. To a solution of 4-dimethylaminobenzaldehyde in 20 mL super dry ethanol sulfisoxazole/sulfamethoxazole was added and was stirred at room temperature for 15 min followed by reflux for 24 h. Yellow-orange precipitate appeared and was filtered, washed with ethanol (3 × 15 mL). The product was dried and crystallized from ethanol at. For both of the compounds, experimental mid-IR spectra were recorded on Perkin Elmer Spectrum 100 FT-IR spectrometer with ATR (Attenuated total reflection) equipment at 4000–400 cm^{-1} region. The C, H, N, and S analyses of the compounds were done on a LECO CHNS 9320 analyzer. Elemental analysis results are presented in Table 1.

COMPUTATIONAL METHOD

The molecular geometry optimizations, nonlinear optical (NLO) activity and vibrational modes were computed by with the help of the Gaussian 09 [17] and Gaussview [18] visualization program. The 6-311G(*d,p*) basis set was used for the all calculations. The geometries were fully optimized without any constraint with the help of an analytical gradient procedure implemented within the Gaussian 09. The molecular structures of the compounds were given in Fig. 1. Vibrational modes and NLO activity were calculated using optimized structures. The fundamental vibrational modes were characterized by their PED (potential energy distribution) obtained by using the VEDA4 program [19]. The calculated frequencies were scaled by 0.9668 to correct the differences between the recorded and calculated data. In the calculation to ^1H and ^{13}C NMR chemical shifts in $CDCl_3$, the GIAO method was used.

RESULTS AND DISCUSSIONS

Conformational Analysis of the Compounds

In this study, the synthesized compounds are conformationally non-rigid molecules with internal rotation. In this case, these molecules can exist in the form of several conformers and so it is necessary to describe the conformational composition of the compounds. In Fig. 2, it is seen four stable conformers of L_1 and L_2. The total energy calculated for the most stable structure of L_1 is −1579.1352 Hartree. For the most stable structure of L_2, the total molecular energy was calculated as −1618.4549 H. The energy differences calculated for each of the conformations are given in Fig. 2 as kcal/mol. For L_1, the energy differences between the conformations have been calculated as 2.53, 2.55, and 4.22 kcal/mol, respectively, for L_2, as 1.87, 1.88, and 2.88 kcal/mol. The energies of the second and third conformers are quite close to each other. All calculations and investigations in the following sections of the paper are made for the most stable versions.

Vibrational Modes of the Compounds

L_1 molecule has 47 atoms and 135 vibrational modes, L_2 has 50 atoms and 144 vibrational modes. They belongs to the point group C_1. Experimental and simulated mid-IR spectra of the compounds were given in Figs. 2 and 3. The selected some important experimental and theoretical vibrational frequencies

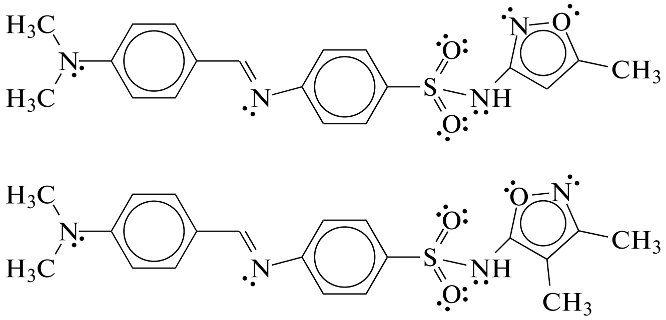

Fig. 1. The molecular structures of L_1 and L_2 in vacuum.

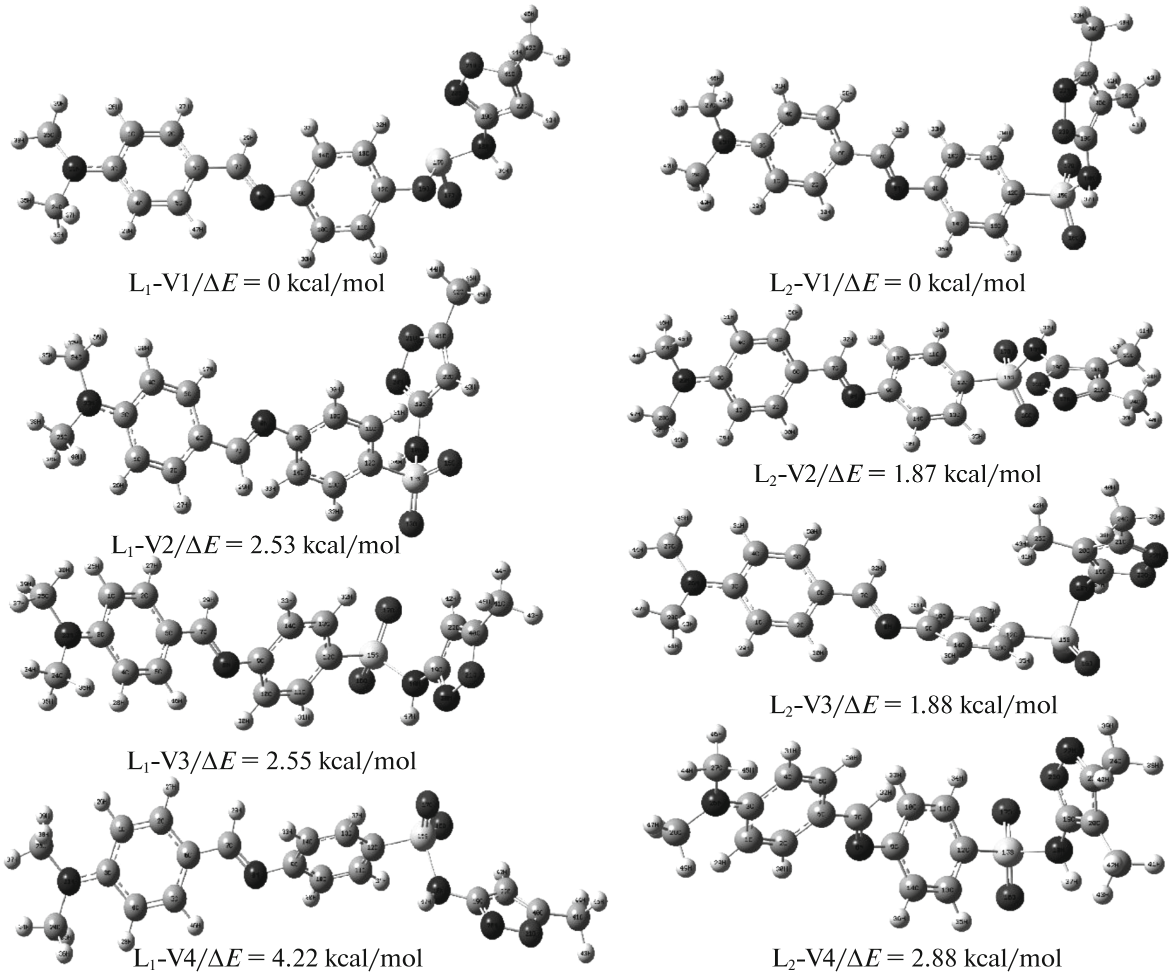

L_1-V1/ΔE = 0 kcal/mol

L_2-V1/ΔE = 0 kcal/mol

L_1-V2/ΔE = 2.53 kcal/mol

L_2-V2/ΔE = 1.87 kcal/mol

L_1-V3/ΔE = 2.55 kcal/mol

L_2-V3/ΔE = 1.88 kcal/mol

L_1-V4/ΔE = 4.22 kcal/mol

L_2-V4/ΔE = 2.88 kcal/mol

Fig. 2. Conformational structures and energy differences of L_1 and L_2 in vacuum.

and IR intensities of the compounds were also given in Tables 2 and 3 together the with PED % assignments.

It is seen from Table 1 that both structures have N–H stretching modes. These vibrations were observed at 3282vw for L_1 and calculated at 3432 cm^{-1}. For L_2, it was recorded at 3382 cm^{-1} and calculated at 3454 cm^{-1}. The main reason for the differences between the calculated and experimental results for both structures is that the calculations are made for a single molecule isolated in the gas phase but the experimental measurements are made in the solid phase and there are too many intermolecular interactions [20].

C–H stretching modes were observed between 2860–3150 cm^{-1} in experimental IR spectra for both structures and these modes were calculated between 2890–3156 cm^{-1} in accordance with experimental results. C–C and C=C stretching vibrations were calculated in the range of 1530–1627 cm^{-1}. These modes are in the range of 1530–1650 cm^{-1} in the experimental spectra. In the literature, these bands are observed between 1400 and 1625 cm^{-1} [21]. These modes are supported by the literature. In previous studies performed, S–O stretching modes have been shown in the range of 1100–1150 cm^{-1} [22]. In this study, while the S–O stretching mode of L_1 was calculated as two bands in 1117 and 1126 cm^{-1}, this mode was calculated as overlapped in 1262 cm^{-1} for L_2. We think that the reason for differences between calculated modes for the two structures is that the placement and position of the isoxazole ring of L_2 are different from that of L_1. Because of this position difference, intermolecular interactions are different for both samples and there are serious differences between the vibration modes. The other important stretching vibrational modes are the N–C stretchings. N–C stretching modes for L_1 were calculated alone at 1627 and 1340 cm^{-1}. In addition, they were calculated at 1600, 1510, and 1486 cm^{-1} in combination with C–C and H–C–C vibrations. In the experimental spectrum, respectively, 1615w, 1333m, 1602w, 1509m, and 1492m were labeled. L_2 for, these modes were calculated alone at 1344 cm^{-1} and were calculated at 1627, 1562 cm^{-1} with the com-

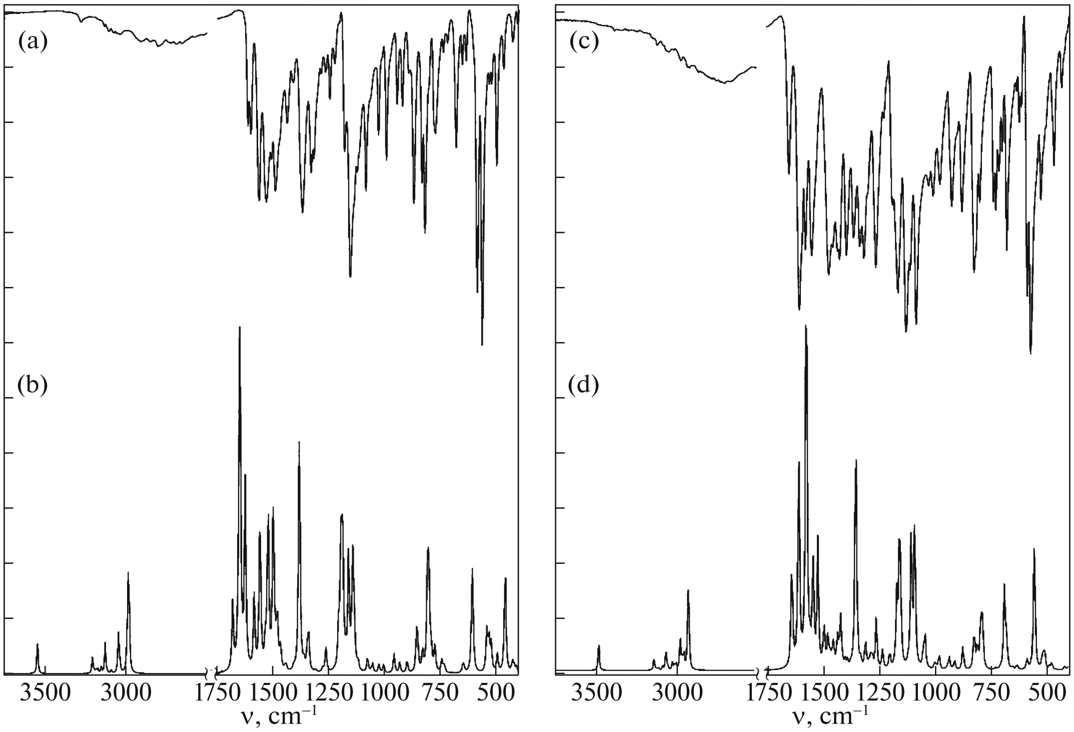

Fig. 3. (a, c) Experimental and (b, d) calculated mid-IR spectra of L_1 (a, b) and of L_2 (c, d).

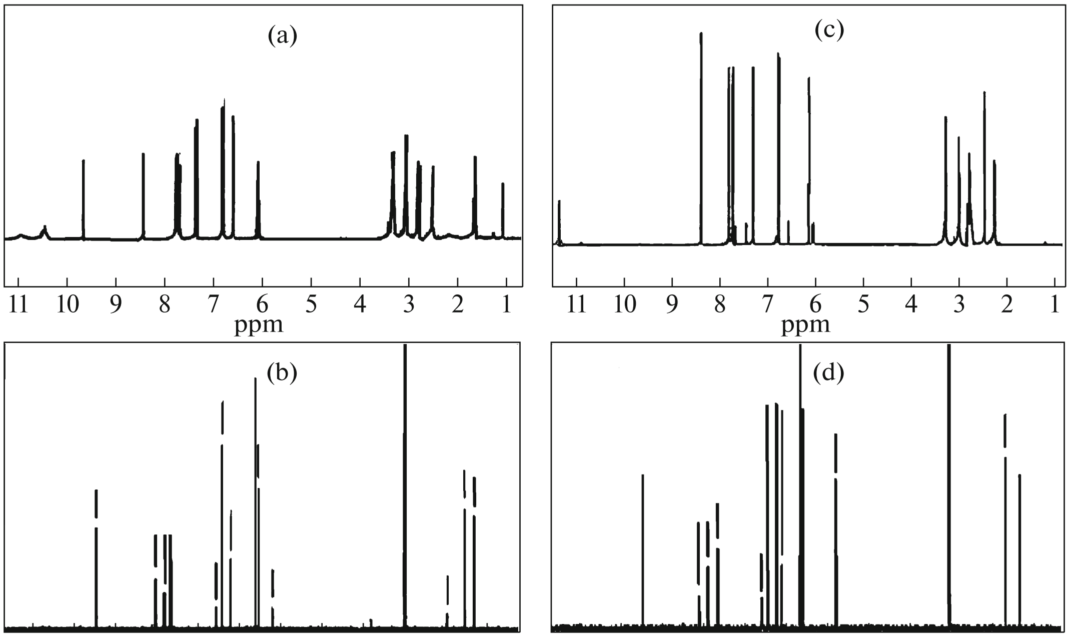

Fig. 4. (a, c) ^{1}H NMR of L_1 (a), L_2 (c); (b, d) ^{13}C NMR of L_1 (b), L_2 (d).

binations of C–C. These bands were observed at 1336s, 1650m, and 1578m in the experimental spectrum. It is also seen from the table that all of the stretching, bending and torsional modes calculated are good agreement with experimental results.

NMR Studies

The NMR spectra (^{1}H–^{13}C) of L_1 and L_2 were measured and interpreted in DMSO. Theoretical NMR calculations were performed with B3LYP/6-

Table 2. Selected experimental and calculated vibrational modes of L_1 (ν, cm^{-1})

Mode	DFT/B3LYP		Exp.	PED, %	Mode	DFT/B3LYP		Exp.	PED, %
	ν	I_{IR}				ν	I_{IR}		
31	420	3.20	407vw	$\delta_{CNC}(13)$	81	1153	43.02	1151sh	$\Gamma_{HCNC}(10)$
34	456	30.57	430w	$\Gamma_{HNCC}(41) + \delta_{OSO}(18)$	82	1158	25.16	1157vs	$\delta_{HCC}(21)$
36	486	8.38	470vw	$\delta_{NCC}(10)$	83	1172	17.70	1182m	$V_{OC}(28) + \delta_{HCC}(27)$
37	512	6.56	501m	$\delta_{CNC}(26)$	85	1225	7.42	1207vw	$V_{NC}(36) + V_{CC}(18)$
38	521	11.05	524w	$\Gamma_{NCCC}(21) + \Gamma_{CCCC}(15)$	86	1228	0.35	1226vw	$V_{OC}(24) + \delta_{HNC}(14) + \delta_{ONC}(13)$
39	531	15.94	535w	$\Gamma_{NNCC}(16) + \Gamma_{NCCC}(11)$	87	1238	1.58	1249w	$\delta_{HCN}(21) + V_{CC}(20) + V_{NC}(13)$
40	592	2.40	567vs	$V_{SO}(17)$	88	1267	0.97	1267vw	$V_{CC}(65)$
41	598	25.01	588vs	$V_{SO}(23) + \delta_{SOC}(13)$	90	1297	11.15	1287vw	$\delta_{HCC}(46) + V_{CC}(12)$
44	634	2.20	638vw	$V_{CC}(37) + \delta_{CCO}(18)$	91	1301	6.28	1305w	$\delta_{HNC}(40) + \delta_{HCC}(16) + \delta_{CCO}(10)$
45	635	0.33	656vw	$\delta_{CCC}(18)$	92	1318	2.69	1321m	$V_{CC}(24)$
46	682	0.60	683w	$\Gamma_{CONC}(37) + \Gamma_{CCON}(21) + \Gamma_{ONCN}(13)$	93	1340	78.73	1333m	$V_{NC}(37)$
49	724	2.44	721vw	$\Gamma_{CCCC}(22)$	94	1361	2.53	1371m	$\delta_{HCN}(54)$
50	760	7.85	740vw	$\Gamma_{HCCC}(77)$	98	1421	7.61	1413w	$V_{CC}(35) + \delta_{HCC}(13)$
51	771	5.42	772sh	$V_{ON}(11) + \Gamma_{ONOS}(11) + V_{NC}(10)$	100	1433	16.08	1417w	$\delta_{HCH}(56)$
52	781	25.05	775w	$V_{OC}(20) + \delta_{CCC}(14)$	104	1450	47.71	1440w	$\delta_{ONC}(15) + \delta_{HNC}(15) + V_{NC}(12)$
53	785	4.17	782w	$V_{SN}(42) + \delta_{ONC}(18)$	105	1468	0.45	1461w	$\delta_{HCH}(54)$
56	809	6.13	808w	$\Gamma_{HCCC}(59) + \Gamma_{HCCN}(13)$	106	1473	55.09	1476sh	$\delta_{HCC}(56)$
57	828	6.89	823s	$V_{CC}(14)$	108	1486	7.26	1492m	$V_{NC}(67)+V_{CC}(13)$
58	834	12.60	836m	$\Gamma_{HCCC}(22) + \delta_{CCC}(10)$	109	1510	48.95	1509m	$V_{NC}(16) + \delta_{HCC}(11)$
59	873	4.18	872m	$V_{CC}(16) + \delta_{CCN}(14) + \delta_{CNC}(11)$	110	1533	22.96	1533m	$V_{CC}(21) + \delta_{CCC}(10)$
60	907	3.41	896vw	$V_{ON}(46) + \delta_{CCO}(15)$	112	1573	53.25	1538m	$V_{CC}(30)$
62	931	5.72	924w	$V_{NC}(47)$	113	1597	100.00	1566m	$V_{CC}(30)$
64	946	0.11	947w	$\Gamma_{HCCC}(80)$	114	1600	24.80	1602w	$V_{CC}(53) + V_{NC}(17)$
67	977	2.09	975vw	$\delta_{CON}(27) + \Gamma_{HCCC}(21) + V_{ON}(16)$	115	1627	19.80	1615w	$V_{NC}(58)$
70	996	1.12	995m	$V_{CC}(23) + \Gamma_{HCCC}(23) + V_{CC}(15)$	117	2890	25.76	2860vw	$V_{CH}(96)$
71	1024	2.72	1030w	$V_{OC}(33) + \delta_{CCO}(25) + V_{NC}(13)$	119	2939	4.02	2917vw	$V_{CH}(100)$
73	1044	5.13	1068w	$\Gamma_{HCNC}(52) + V_{NC}(32)$	126	3051	2.24	3043vw	$V_{CH}(97)$
74	1083	2.89	1087m	$\delta_{HCC}(55) + V_{CC}(13)$	131	3094	1.15	3086vw	$V_{CH}(99)$
77	1110	3.36	1117sh	$V_{SO}(52) + \delta_{HCC}(20)$	133	3104	3.53	3120vw	$V_{CH}(87)$
79	1132	37.52	1126m	$V_{SO}(29) + \delta_{HCC}(26)$	134	3156	0.06	3143vw	$V_{CH}(99)$
80	1140	25.02	1142sh	$\delta_{HCC}(43)$	135	3432	10.13	3282vw	$V_{NH}(100)$

Table 3. Selected experimental and calculated vibrational modes of L_2 (ν, cm^{-1})

Mode	DFT/B3LYP		Exp.	PED, %	Mode	DFT/B3LYP		Exp.	PED, %
	ν	I_{IR}				ν	I_{IR}		
33	408	0.10	414vw	Γ_{HCCC}(72)	82	1112	0.77	1112s	δ_{HCC}(39) + V_{CC}(26)
34	419	0.59	430vw	Γ_{HCCC}(15) + δ_{HCC}(14)	83	1147	25.64	1132vs	V_{CC}(43)
35	424	0.16	438w	Γ_{HCCC}(55)	84	1151	11.49		δ_{HCC}(23)
36	460	0.15	472m	δ_{HCC}(41)	86	1160	13.33	1167s	δ_{HCC}(52) + V_{CC}(10)
37	476	1.75	477sh	δ_{HCC}(21)	87	1193	4.48	1192m	δ_{HCC}(20) + V_{CC}(15)
39	509	3.70	509sh	δ_{HCC}(23)	88	1226	4.17	1228w	V_{CC}(56) + δ_{HCN}(12)
40	519	2.78	518sh	δ_{HCC}(30) + Γ_{HCCC}(10)	90	1262	7.30	1265s	V_{SO}(68)
41	524	0.89	530m	Γ_{HCCC}(52)	94	1298	6.72	1301sh	δ_{HCC}(38) + V_{CC}(10)
42	555	9.55	556sh	Γ_{HCCC}(23)	95	1321	1.63	1317s	V_{CC}(40)
43	557	21.43	576vs	δ_{HCC}(33)	97	1344	50.78	1336s	V_{NC}(38)
44	588	2.95	592s	V_{CC}(10)	98	1363	0.95	1362s	δ_{HCC}(38)
45	622	0.03	618w	δ_{HCC}(57)	102	1402	1.16	1395s	δ_{HCN}(47) + δ_{HCH}(29)
46	630	0.06	626w	δ_{HCC}(27)	104	1423	6.67	1426s	V_{CC}(22) + δ_{HCN}(13) + δ_{HCC}(13)
47	634	1.00	640w	δ_{HCC}(32)	109	1443	3.61	1435s	δ_{HCC}(58)
49	680	3.58	673sh	δ_{HCC}(12) + Γ_{HNSC}(11) + Γ_{HNCC}(10)	112	1465	6.22	1456s	δ_{HCC}(36) + $_{VCC}$(12)
50	687	22.00	682s	V_{CC}(56)	114	1482	9.52	1474s	δ_{HCC}(67)
51	700	1.15	703w	Γ_{HNSC}(23)	117	1531	25.40	1549s	V_{CC}(48)
52	721	0.09	717m	Γ_{HCCC}(69)	119	1562	100.00	1578s	V_{CC}(57) + V_{NC}(18)
53	725	0.34	731m	V_{CC}(29) + δ_{HCC}(12)	120	1596	51.34	1604vs	V_{CC}(58) + δ_{HCC}(11)
54	782	10.90	741m	δ_{HNS}(30)	121	1625	16.32	1650m	V_{CC}(63)
56	793	13.85	783sh	V_{CC}(30) + δ_{HCH}(16)	122	1627	9.66		V_{CC}(21) + V_{NC}(19)
58	808	3.85	803m	Γ_{HCCC}(13)	124	2897	10.92	2859w	V_{CH}(79)
59	819	6.34	821sh	V_{CC}(39) + δ_{HCC}(10)	126	2921	3.80	2914vw	V_{CH}(97)
60	821	4.69	828s	Γ_{HCCC}(21) + Γ_{HCCN}(15)	127	2932	2.46	2930vw	V_{CH}(100)
61	869	5.79	882m	δ_{HCC}(46)	130	2970	1.79	2971vw	V_{CH}(97)
62	908	2.65	907w	V_{CC}(47)	135	3034	5.02	3013vw	V_{CH}(94)
64	931	2.64	927m	V_{CC}(45)	140	3097	0.13	3042vw	V_{CH}(99)
69	977	3.52	980m	Γ_{HCCC}(42) + Γ_{HCNC}(37)	141	3105	1.32	3062vw	V_{CH}(95)
73	1018	0.19	1010m	δ_{HCC}(69)	142	3107	1.81	3080vw	V_{CH}(99)
74	1038	0.10	1030m	V_{CC}(48) + δ_{HCC}(11)	143	3108	0.07	3117vw	V_{CH}(94)
77	1086	26.79	1067sh	V_{CC}(59)	144	3454	5.90	3382vw	V_{NH}(100)
79	1098	36.38	1085vs	δ_{HNS}(46)					

311G(*d,p*) level of theory in DMSO phase. Isotropic shielding tensors of ^{13}C were changed into chemical shifts by using a linear relationship suggested by Blanco et al. [23]. A similar relationship proposed by Silva et al. [24] was used to obtain chemical shifts for ^{1}H. The computed chemical shift values fit well with experimental values. The experimental and calculated chemical shift values are shown in Table 4. The ^{13}C

Table 4. The experimental and theoretical ^{1}H and ^{13}C NMR chemical shifts (δ, ppm) for ligands

	L_1		L_2			L_1		L_2	
	δ(exp.)	δ(calc.)	δ(exp.)	δ(calc.)		δ(exp.)	δ(calc.)	δ(exp.)	δ(calc.)
C1	10.76(CH_3)	10.90	10.56	10.67	C19–20	19.00(NCH_3)	19.22	12.48	12.78
C2	161.63	161.28	162.75	162.83	H1	1.63	1.77	2.28	2.19
C3	129.12	129.33	121.97	121.76	H4	1.04	1.07	—	—
C4	6.26(CH_3)	6.11	—	—	H3	6.05	6.11	6.06	6.03
C5	161.64	161.26	154.66	154.38	NCH_3	3.025	3.64	3.02	3.02
C6	154.66	154.02	153.72	154.21	NCH_3	2.95	2.76	2.98	2.91
C7	124.12	124.66	123.61	123.36	H7	6.77	6.89	7.44	7.48
C8	113.08	112.87	124.98	124.44	H8	7.31	7.18	7.79	7.68
C9	111.32	111.51	95.73	96.21	H9	7.34	7.51	6.77	6.82
C10	124.12	124.16	113.09	112.08	H10	7.67	7.44	6.13	6.09
C11	156.73	156.28	158.39	158.14	H12	8.41	8.78	8.38	8.45
C12	190.30(CN=N)	190.44	190.30	191.27	H15–H16	6.26	6.26	7.73	7.63
C13	104.71	103.18	111.87	111.43	H17–H16	6.57	6.43	6.06	6.05
C14–C15	131.99	132.23	131.98	131.30	H18	7.75	7.96	—	—
C16–C17	129.12	128.59	95.86	95.48	NH	9.65	9.47	11.32	10.88
C18	104.71	104.68	129.57	129.88					

NMR and ^{1}H NMR spectrums of the Schiff bases in DMSO are given in Fig. 4.

In the ^{1}H NMR spectrum of L_1; H1, H4, H12, and $N(CH_3)_2$ protons appeared at 1.63, 1.04, 8.41, and 3.83–2.95 ppm were calculated at 1.77, 1.07, 8.78, and 3.64–2.76 ppm. A signal were also observed at δ = 9.65 ppm of the N–H-group (calculated at 9.47 ppm). Signals in the range of δ = 6.26–7.75 ppm region belong to aromatic Ar–H protons. In ^{13}C-NMR spectra of L_1; C1, C4, C12, and $N(CH_3)_2$ carbon signals are assigned at 10.76, 6.26, 190.30, and 19.00 ppm (calculated 10.90, 6.11, 190.44, and 19.22 ppm), respectively. Signals in the range of δ = 104.70–162.36 ppm region belong to aromatic Ar–C carbons.

In the ^{1}H NMR spectrum of L_2; H1, H12, and $N(CH_3)_2$ protons appeared at 2.28, 8.38, and 3.02–2.89 ppm were calculated at 2.19, 8.38, and 3.02–2.91 ppm. A signal were also observed at δ = 11.32 ppm of the of the N–H-group (calculated at 10.88 ppm). Signals in the range of δ = 6.06–7.79 ppm region belong to aromatic Ar–H protons. In ^{13}C-NMR spectra of L_2; C1, C12, and $N(CH_3)_2$ carbon signals are assigned at 10.56, 190.30, and 12.48 ppm (calculated 10.67, 191.27, and 12.78 ppm), respectively. Signals in the range of δ = 95.73–162.75 ppm region belong to aromatic Ar–C carbons.

Nonlinear Optical Properties (NLO)

The optical properties of matter can be expressed as the response of the electrons to the electric field. As it is known, the electric field component of the light sent to the material poles that substance. The polarity of an atom or molecule is a measure of how easily the nucleus and electrons can shift from their equilibrium states. The reaction of an isolated molecule against an applied external electric field results in a reshaping of the dipole moment of the molecule:

$$\mu_t = \mu_0 + \alpha_{ij}E_i + \beta_{ijk}E_iE_j + \ldots, \tag{1}$$

where μ is called the permanent dipole moment of the molecule, α is the linear polarizability, β_{ijk} is first order hyperpolarizability tensor components. First order hyperpolarizability is quantities that affect the nonlinear optical performance of matter. The mean polarizability $\langle\alpha\rangle$ is defined as [25]:

$$\langle\alpha\rangle = 1/3(\alpha_{xx} + \alpha_{yy} + \alpha_{zz}). \tag{2}$$

The calculation of first order hyperpolarizability from output given as follows [26]:

$$\begin{aligned}\beta_{\text{tot}} = [(\beta_{xxx} + \beta_{xyy} + \beta_{xzz})^2 + (\beta_{yyy} + \beta_{yzz} + \beta_{yxx})^2 \\ + (\beta_{zzz} + \beta_{zxx} + \beta_{zyy})^2]^{1/2}.\end{aligned} \tag{3}$$

Table 5. The electric dipole moment (μ, D), the mean polarizability ($\langle\alpha\rangle \times 10^{24}$, esu) and the first hyperpolarizability ($\beta_{tot} \times 10^{33}$, esu) of L_1 and L_2

Parameter	L_1	L_2	Parameter	L_1	L_2
μ_x	−6.3783	2.4938	β_{xxx}	76964.76	−43518.13
μ_y	3.1339	4.8305	β_{xxy}	−12207.33	−9129.41
μ_z	−2.4890	−0.1934	β_{xyy}	242.76	714.90
M	7.5299	5.4396	β_{yyy}	1687.08	518.10
α_{xx}	87.14	82.63	β_{xxz}	−138.66	2142.63
α_{xy}	−4.40	4.37	β_{xyz}	190.58	280.17
α_{yy}	35.88	39.65	β_{yyz}	264.71	183.84
α_{xz}	1.17	1.40	β_{xzz}	−2599.48	1613.56
α_{yz}	2.09	2.42	β_{yzz}	898.14	164.50
α_{zz}	35.78	31.31	β_{zzz}	−914.21	1092.27
$\langle\alpha\rangle$	52.93	51.19	β_{tot}	75230.07	42185.70

α: 1 a.u. = 0.1482×10^{-24} esu.
β: 1 a.u. = 8.6393×10^{-33} esu.

The calculated dipole moment μ, mean polarizability $\langle\alpha\rangle$, first order hyperpolarizability β_{tot} are reported in the Table 5.

First order hyperpolarizability of L_1 and L_2 was computed to be 75.23×10^{-30} and 42.18×10^{-30} esu, respectively. Urea is reference molecule for classification of good NLO organic molecules. It found that, the first order hyperpolarizabilities of L_1 and L_2 are 201.79 and 113.14 times larger than that of urea (0.3728×10^{-30} esu), respectively. According to evaluated results, the L_1 and L_2 present large nonlinear optical activity and are candidate molecules for nonlinear optical applications.

CONCLUSION

As a result of this study, the following decisions were obtained. Two new Schiff bases compounds L_1 and L_2 were synthesized and their structures were elucidated using elemental analysis and spectroscopic methods. Estimated structures of synthesized compounds were drawn in 3D and optimizations were performed. Based on optimized structures, theoretical vibrational modes, ^{1}H and ^{13}C NMR and NLO calculations were done. The all calculated parameters were compared with the experimental ones and the structures of the compounds have clarified. Intermolecular hydrogen bond interactions causes serious differences between calculated and experimental N–H stretching vibrational modes. The first order hyperpolarizabilities of L_1 and L_2 are 201.79 and 113.14 times larger than that of urea (0.3728×10^{-30} esu). The compounds present large nonlinear optical activity.

REFERENCES

1. Z. H. Chohan, H. A. Shad, and F. H. Nasim, Appl. Organomet. Chem. **23**, 319 (2009).
2. A. E. Boyd, Diabetes. **37**, 847 (1988).
3. R. Kasımogulları, M. Bülbül, et al., Eur. J. Med. Chem. **45**, 4769 (2010).
4. L. de Luca, S. Ferro, F. M. Damiano, et al., Eur. J. Med. Chem. **71**, 105 (2014).
5. A. D. Wright, M. H. Winterborn, P. J. Forster, J. P. Delamere, G. L. Harrison, and A. R. Bradwell, J. Wilderness Med. **5**, 49 (1994).
6. L. Sun, Y. Wu, Y. Liu, X. Chen, and L. Hu, Bioorg. Med. Chem. Lett. **27**, 261 (2017).
7. H. Yoshino, N. Ueda, et al., J. Med. Chem. **35**, 2496 (1992).
8. C. T. Supuran, Expert Opin. Drug Disc. **12**, 61 (2017).
9. N. Özbek, H. Katırcıoglu, N. Karacan, and T. Baykal, Bioorg. Med. Chem. **15**, 5105 (2007).
10. N. Özbek, S. Alyar, H. Alyar, E. Sahin, and N. Karacan, Spectrochim. Acta, Part A **108**, 123 (2013).
11. F. Akyıldız, S. Alyar, M. T. Bilkan, and H. Alyar, J. Mol. Struct. **1174**, 160 (2018).
12. S. Alyar, T. Şen, Ü. Ö. Özmen, H. Alyar, S. Adem, and C. Şen, J. Mol. Struct. **1185**, 416 (2019).
13. U. Özdemir, N. Karacan, O.S. Senturk, S. Sert, and F. Uğur, Synth. React. Inorg. Metal.-Org. Chem. **34**, 1057 (2004).
14. N. Özbek, S. Alyar, and N. Karacan, J. Mol. Struct. **938**, 48 (2009).
15. A.B. Gündüzalp, Ü. Ö. Özmen, et al., Med. Chem. Res. **23**, 3255 (2014).

16. N. Özbek, G. Kavak, Y. Özcan, S. Ide, and N. Karacan, J. Mol. Struct. **919**, 154 (2009).
17. M. J. Frisch et al., *Gaussian 09, Revision B.01* (Gaussian Inc., C.T. Wallingford, 2009).
18. R. D. Dennington, T. A. Keith, and J. M. Millam, *GaussView 5* (Gaussian, Inc., 2008).
19. M. H. Jamróz, *Vibrational Energy Distribution Analysis* (VEDA 4, Warsaw, 2004).
20. M. T. Bilkan, J. Mol. Liq. **238**, 523 (2017).
21. M. T. Bilkan, Russ. J. Phys. Chem. A **92**, 1920 (2018).
22. A. Mahmood, T. Akram, and E. B. de Lima, J. Mol. Struct. **1108**, 496 (2016).
23. F. Blanco, I. Alkorta, and J. Elguero, Magn. Reson. Chem. **45**, 797 (2007).
24. A. M. S. Silva, R. M. S. Sousa, M. L. Jimeno, F. Blanco, I. Alkorta, and J. Elguero, Magn. Reson. Chem. **46**, 859 (2008).
25. H. Soscun, O. Castellano, et al., J. Mol. Struct.: THEOCHEM **592**, 19 (2002).
26. K. S. Thanthiriwatte and K. M. Nalin de Silva, J. Mol. Struct.: THEOCHEM **617**, 169 (2002).